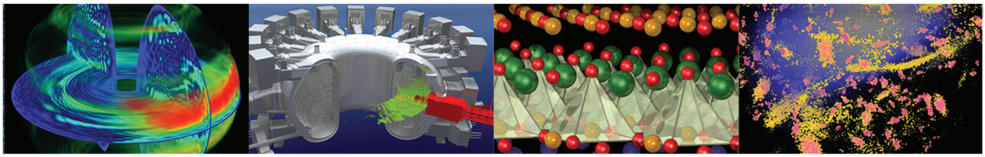

SciDAC 2010

Electronic Visualization and Poster Night

July 14
Chattanooga
Tennessee

U.S. DEPARTMENT OF ENERGY
Office of Science

Scientific Discovery through Advanced Computing

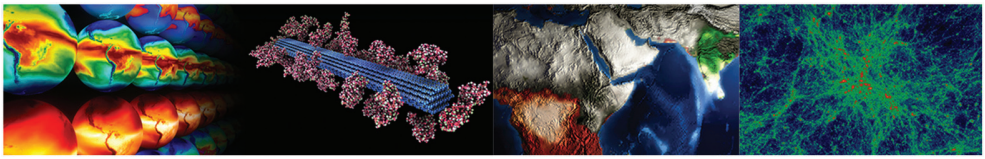

Type Ia Supernova: Turbulent Combustion on the Grandest Scale

Hank Childs, Haitao Ma, Stan Woosley, John Bell, Ann Almgren, Andy Nonaka

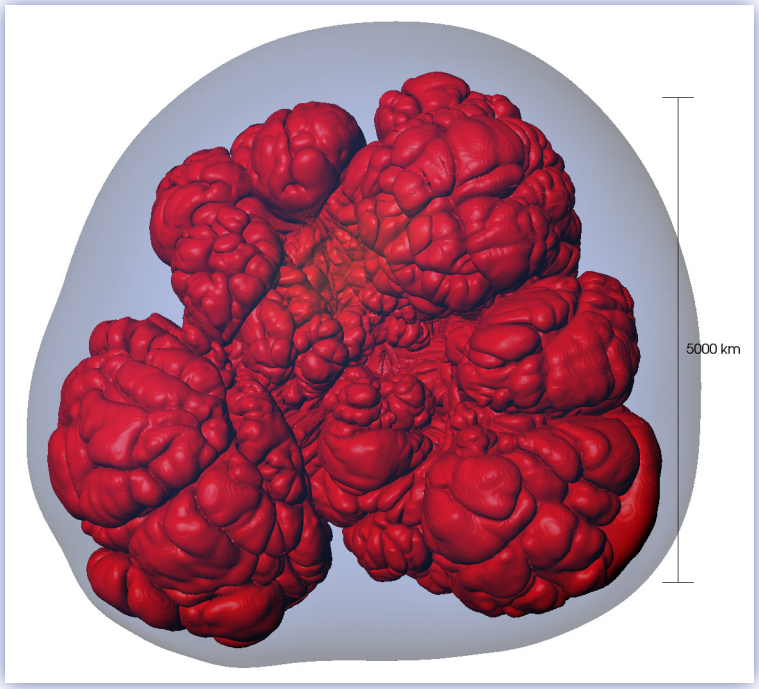

This image shows the star surface (light blue) and the flame front (red) inside of a Type Ia supernova simulation.

Video description:

Deep inside a dying star in a galaxy far, far away, a carbon fusion flame ignites. Ignition may happen in the middle or displaced slightly to one side, but this simulation explores the consequences of central ignition. In a localized hot spot, represented here by a deformed sphere with an average radius of 100 km, carbon is assumed to have already fused to iron, producing hot ash (~ten billion K) with a density about 20% less than its surroundings. As the burning progresses, this hot buoyant ash rises up and interacts with cold fuel. Rayleigh-Taylor fingers give rise to shear and turbulence, which interacts with the flame, causing it to move faster. In about two seconds, the energy released blows the entire white dwarf star up, leaving nothing behind but a rapidly expanding cloud of radioactive nickel, iron, and other heavy elements. A Type Ia supernova is born.

Dual-Space Visual Analysis of a Direct Numerical Simulation of Lifted Turbulent Jet Flames

Simulation
Chun Sang Yoo, Edward Richardson, Ramanan Sankaran, Jacqueline H. Chen

Visualization
Hongfeng Yu, Jishang Wei, Ray W. Grout, Kwan-Liu Ma

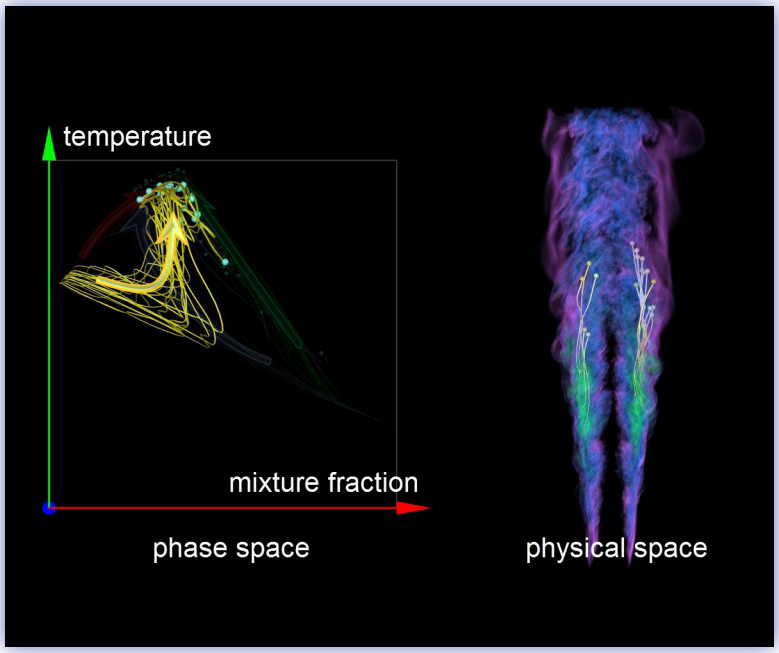

Dual-Space Visual Analysis of a Direct Numerical Simulation of Lifted Turbulent Jet Flames

Video description:
Recent combustion simulations of a turbulent lifted autoignitive ethylene/air jet flame were instrumented with particles originating in both the fuel and oxidizer streams. The particle trajectories provide lagrangian statistics correlating temperature and mixture fraction, two key combustion parameters, encapsulating the unsteadiness associated with turbulent mixing and autoignition. The following visualization shows time-varying particles and how they are clustered into groups with distinct characteristics. The relationship between the particle trajectories in phase and physical space is highlighted by the linked images and provides combustion scientists with detailed information regarding the evolution of fluid parcels traversing a turbulent autoignitive environment.

Searching for Baryon Acoustic Oscillations in Intergalactic Absorption, The Expanding Universe

Science
Michael L. Norman, Robert Harkness, Pascal Paschos, Rick Wagner

Visualization
Mark Hereld, Joseph A. Insley, Eric C. Olson, Michael E. Papka

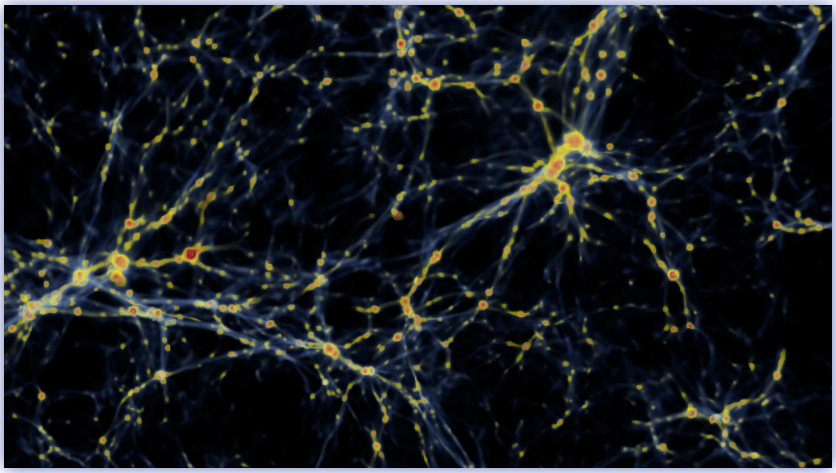

This figure shows the density field of the baryon acoustic oscillations simulation, illustrating the gravitational clumping that occurs even as the volume continues to expand.

Video description:

This simulation follows the growth of density perturbations in both gas and dark matter components in a volume 1 billion light years on a side beginning shortly after the Big Bang and evolved to half the present age of the universe. It calculates the gravitational clumping of intergalactic gas and dark matter modeled using a computational grid of 64 billion cells and 64 billion dark matter particles. The simulation uses a computational grid of 4096^3 cells and took over 4,000,000 CPU hours to complete.

The visualization shows the density value, whose range spans over 6 orders of magnitude. The animation illustrates the expansion of the universe over time, and highlights how individual structures (such as galaxy clusters) collapse due to gravity, while simultaneously being pushed further and further from each other. The animation was made from 148 terabytes of data generated on Kraken at the National Institute for Computational Sciences and transferred to Argonne over ESnet. The rendering was performed on Eureka at the Argonne Leadership Computing Facility.

iMageVis3D Mobile

4

Tom Fogal, Jens Krueger, Chems Touati

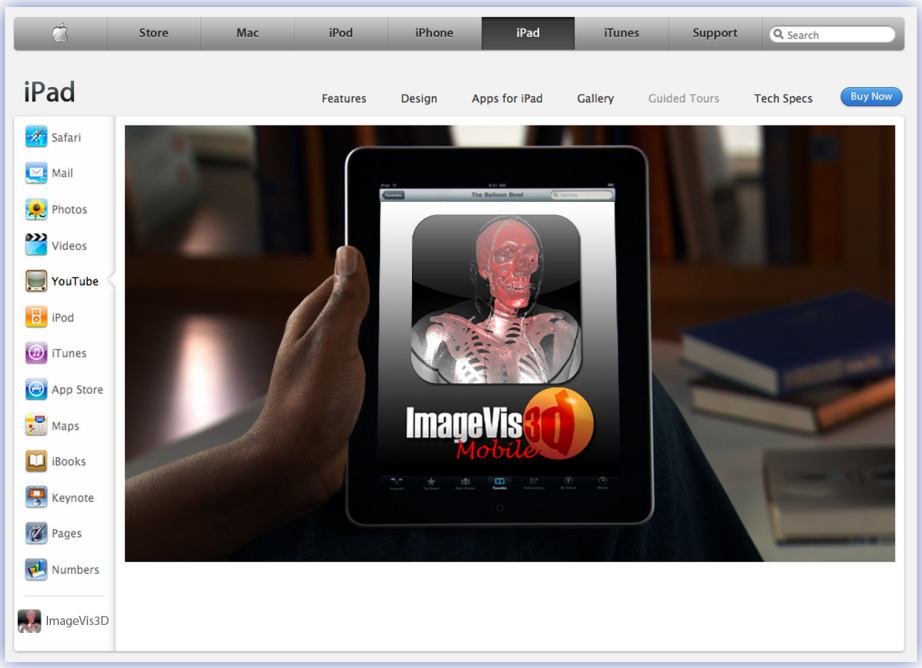

ImageVis3D mobile is a mobile volume rendering application that allows one to visualize and share your data while you are on the go.

Video description:

While mobile visualization is a popular field, due to the high computational cost there has been relatively little work investigating volume rendering on mobile devices. ImageVis3D mobile succeeds in providing interactive renderings which clearly detail the features of a data set. The tool makes it easy for you and your colleagues to set up collaboration-specific networks to distribute and visualize data with ease.

Amit Chourasia, Emmett Mcquinn, Bernard Minster, Jurgen Schulze, Geoffrey Ely, Kim Olsen, Yifeng Cui, Alexei Kritsuk, Sergey Ustyugov, Mike Norman, Kim Olsen, Steve Day, Thomas Jordan

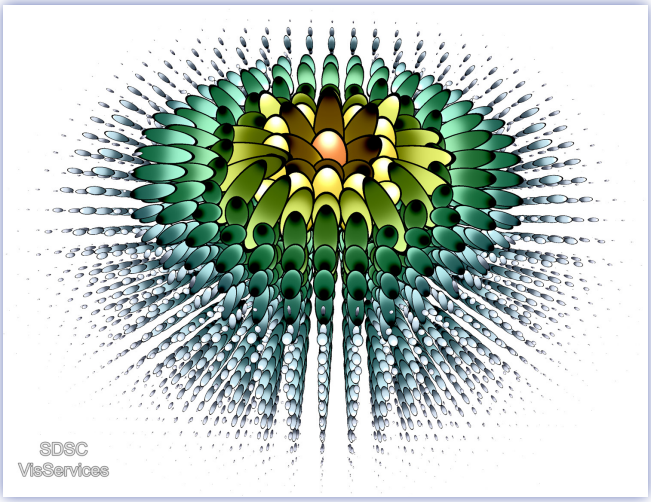

The figure shows velocity field for a point source earthquake simulation where the size and color of ellipsoidal glyph indicate velocity magnitude. Vector orientation is encoded as a white and a black spot on the pole of the ellipsoid, where the white spot indicates the vector direction towards the viewer and black spot away from the viewer.

Video description:

Vector visualization is an important area to investigate scientific data in many domains. Prior visualization strategies have primarily focused on maps and volumetric rendering of scalar fields, which do not permit a full characterization of underlying phenomena. We have developed an interactive glyph visualization application that allows scientists to explore vector fields. We implement novel technique of procedural dipole and cross mark texturing to encode and display vector data. We employ a novel lattice method to show neighborhood, which also enables to distinguish glyphs. We further enhance visualization by using screen space ambient occlusion, jitter, outline halos and displacement. By combining contextual information with glyphs, such as geographic maps and representations of crustal structure with three-dimensional isosurfaces, scientists are able examine vector fields in a rich and interactive multivariate environment. We demonstrate the results for time-dependent vector data from three different simulations.

The Convective Phase Preceding Type Ia Supernovae Explosions

M. Zingale, A. S. Almgren, J. B. Bell, C. M. Malone, A. Nonaka, G. H. Weber, S. E. Woosley

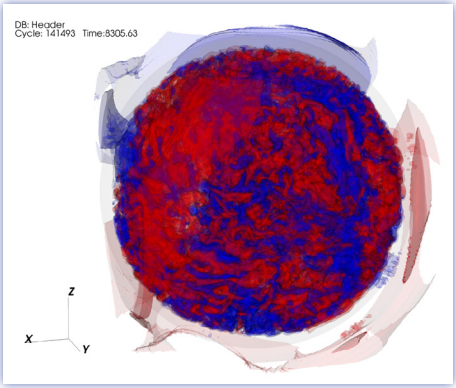

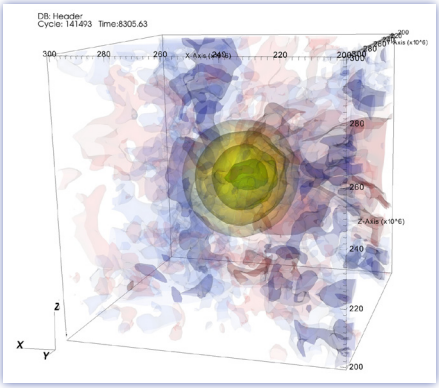

MAESTRO simulation of the final hours of convection in a white dwarf preceding the explosion of a Type Ia supernova. The movie shows the radial velocity (red and blue contours) and the nuclear energy generation (yellow/green/purple contours). The right panel shows the inner 1000 km^3.

Video description:

Type Ia supernovae are believed to result from the thermonuclear explosion of a Chandrasekhar mass white dwarf. For centuries preceding the ignition, carbon fusion reactions at the center drive convection throughout the star. The details of this convection are important to understanding the subsequent explosion. We used the low Mach number hydrodynamics code, MAESTRO, to model the last hours of convection preceding the ignition. During this convective phase, buoyant plumes rise outward from the center, cooling via expansion. The simulation ends when this expansion can no longer quench the burning and a flame front is born (ignition). The low Mach number hydrodynamics algorithm was critical to performing this simulation, as the flow is highly subsonic, putting it out of reach of traditional hydrodynamics codes.

Electromagnetic Wake in an Energy Recovery Linac Vacuum Chamber with Moving Simulation Window

Greg Schussman, Rich Lee, Liling Xiao, Cho-Kuen Ng, Ken Moreland

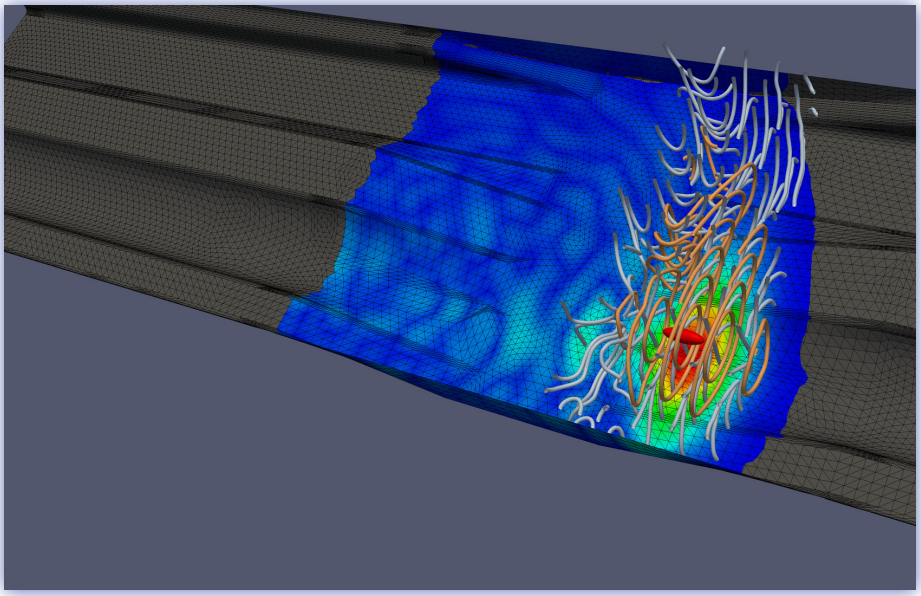

Electromagnetic wakefields from simulation of a short electron bunch in a Vacuum Chamber of the Energy Recovery Linear Accelerator.

Video description:

This animation shows electromagnetic wakefields from a short electron bunch traveling through a Vacuum Chamber of the Energy Recovery Linac. Short bunches require such a fine mesh for accuracy that simulation size becomes excessive. In this simulation, computation was limited to only the volume within a moving window surrounding the bunch. When the bunch has moved sufficiently far, the window jumps forward.

An oversized red pill represents the 0.3 mm bunch. On the surface pseudo-coloring shows the electric field strength, with uncomputed values (outside the moving window) or zero values both shown as grey and low through high values shown as rainbow colors, blue through red. Only the coarse mesh is shown because this resolution is insufficient for extremely fine details. Electric field lines are shown in pale blue. Magnetic field lines form loops and are shown in light orange. This animation was rendered in ParaView.

Verification Study of Buoyancy-Driven Turbulent Nuclear Combustion for Three Different Physical Situations

8

Ray Bair, Anshu Dubey, Robert Fishe, Jonathan Gallagher, Randy Hudson, Don Lamb, Dongwook Lee, John Norris, Mike Papka, Katherine Riley, Dean Townsley

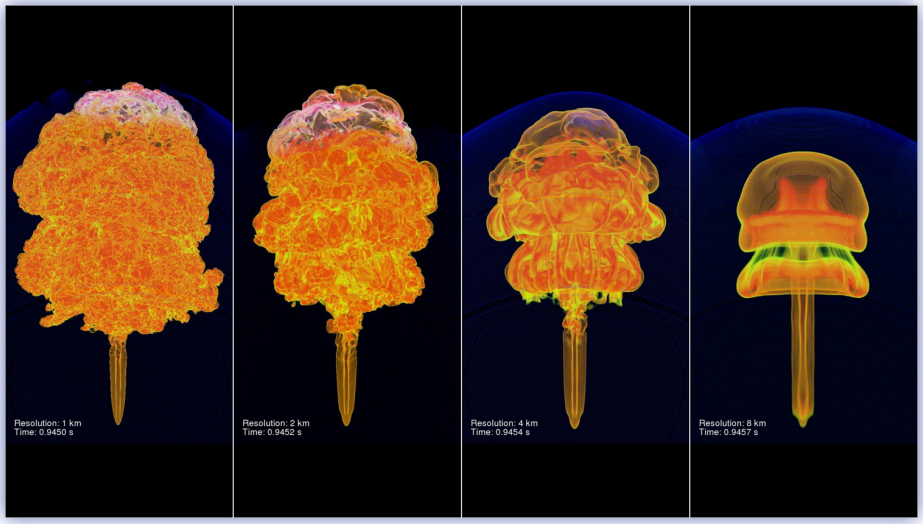

Understanding how Buoyancy-driven turbulent nuclear combustion occurs in different physical situations is a key component to understanding the energy dynamics of the deflagration phase of Type Ia supernovae.

Video desription:

Buoyancy-driven turbulent nuclear combustion determines the rate of nuclear burning during the deflagration phase (i.e., the ordinary nuclear flame phase) of Type Ia supernovae, and hence the amount of nuclear energy released during this phase. It therefore determines the amount the white dwarf star expands prior to initiation of a detonation wave, and so the amount of radioactive nickel and thus the peak luminosity of the explosion. However, this key physical process is not fully understood. To better understand this process, the Flash Center has conducted an extensive series of large-scale 3D simulations of buoyancy-driven turbulent nuclear combustion for three different physical situations. This movie shows the results for some of these simulations.

Hybrid Particle Finite Element Simulation of Impact, Perforation, and Fragmentation

Randall Hand, Miguel Valenciano, Eric Fahrenthold, Kwon Joong Son

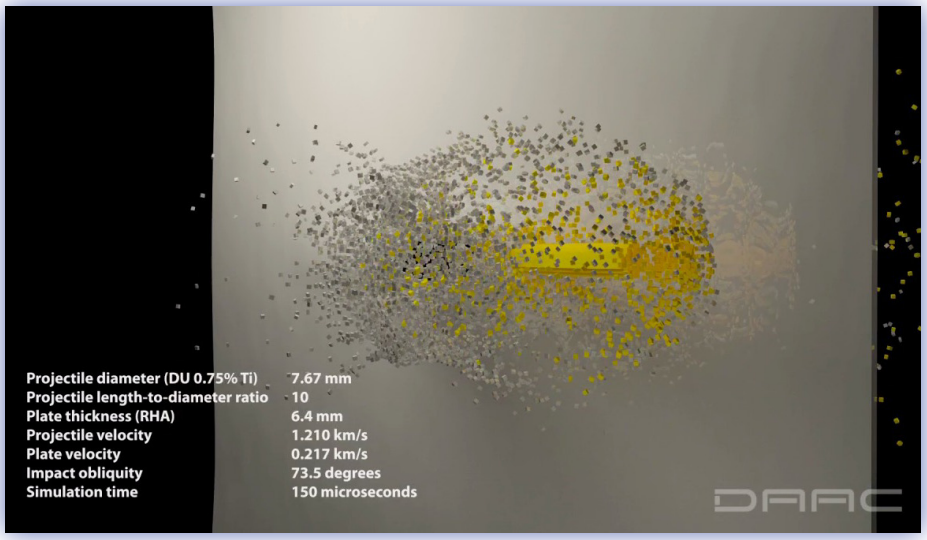

A 7.67mm rod projectile impacting a 6.4mm plate at 1.21 km/s.

Video description:

The 2 simulations model impact experiments conducted at the University of Dayton and Los Alamos National Laboratory. The simulations employ a hybrid particle finite-element method and the parallel code EXOS, both developed at the University of Texas at Austin.

Turbulence-Flame Interaction of Initial Sparks of a Type Ia Supernova

Alan C. Calder, Aaron P. Jackson, Dean M. Townsley

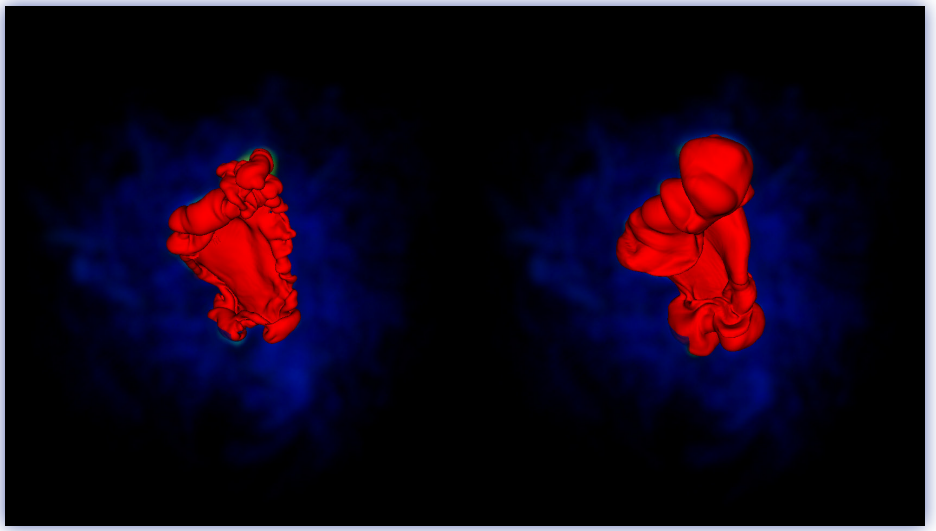

The evolution of the first sparks (red) of a thermonuclear supernova interacting with a turbulent velocity field (blue). A model of the turbulence-flame interaction (TFI) utilizing a local measure of the turbulent velocity was developed (right) and compared to an indirect treatment of the TFI using only buoyancy effects (left). We find that our local treatment of TFI produces a larger enhancement to the flame speed as indicated by a larger volume enclosed by the flame surfac.

Video description:

Type Ia supernovae are bright stellar explosions thought to occur when a runaway thermonuclear reaction incinerates a compact star known as white dwarf. In many models, the explosion begins with a flame born in the turbulent environment near the center of the white dwarf. The effect of turbulence on the evolution of the nascent flame is incompletely understood and is the subject of active research. We present two simulations of the early flame evolution in a supernova. One incorporates a physically-motivated turbulence-flame interaction model that utilizes a local measure of the turbulence, while the other relies only on indirect buoyancy effects. In the renderings, the red isosurface represents the flame front and the blue volume rendered features the magnitude of the vorticity of the turbulent flow. The enhanced flame speed of the local interaction may be observed as the increased volume of burned material enclosed by the isosurface.

Computational Study of the Molecular Mechanism of Alzheimer's Disease

Igor F. Tsigelny, Yuriy Sharikov, Eliezer Masliah

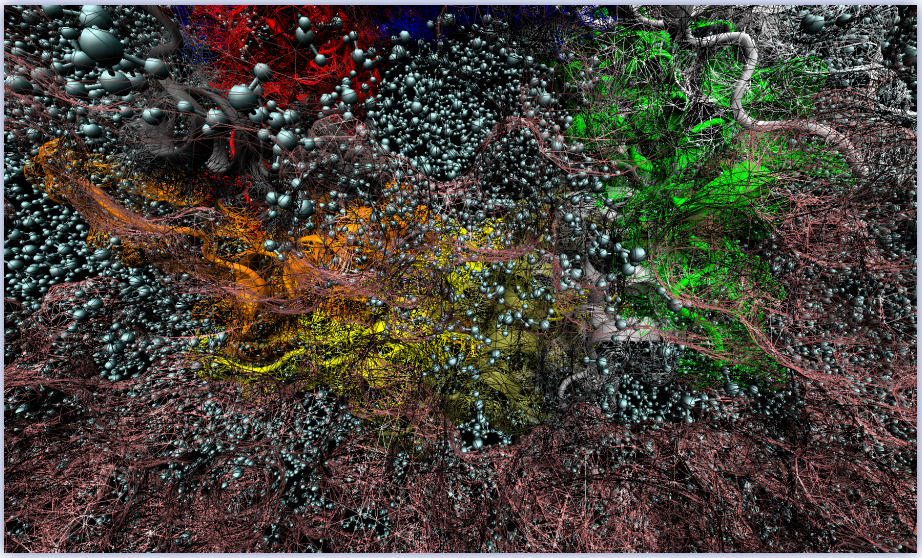

Video description:

In our study we conducted all atom molecular dynamic simulations of the full-length amyloid beta 1-42 (Aβ) peptide, then studied possible annular oligomer aggregates formed by different typical conformers of Aβ. The various annular aggregates are possible to be formed. Our study of the aggregates having the best energy contacts between themselves and with the membrane brought a limited number of them for further study. These aggregates were situated on the membrane and molecular dynamic simulations of the system have been conducted. The provided images show the possible penetration of the Aβ aggregates to the membrane with the membrane perforation. Such pores can lead to uncontrolled influx of various ions to the neuronsl, including Calcium 2+ ions, that can trigger the signaling cascade of cell death. The damage and death of these neurons is associated with the Alzheimer's disease.

Large-Scale Volumetric Visualization of Doppler Reflectivity Data

Peter Kristof, Jin Ryong Kim, Bedrich Benes, Lan Zhao, Carol X. Song

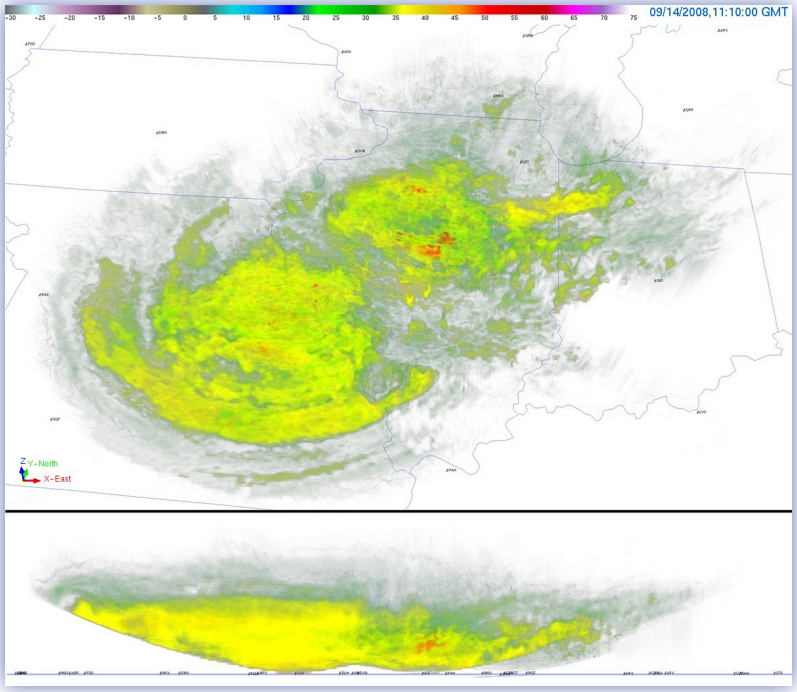

Volumetric visualization of Hurricane Ike, which occurred in Indiana and Illinois states on September 14, 2008, with visualization importance given to medium to heavy rainfall regions.

Video description:

The super resolution NEXRAD (Next-Generation Radar) Level II data, aka Weather Surveillance Doppler Radar 1988 (WSR-88D) data, provides critical information on reflectivity, wind velocity and spectrum width for the entire United States. The goal of this work is to develop a framework that enables multiple users to interactively access, analyze and visualize the Doppler reflectivity data in 3D to study near real-time weather events. To provide interactive high-quality volumetric weather visualization, we combined two approaches dealing with large-scale storage of global weather data and out-of-core volume rendering using CUDA ray casting. The results of our work show that the reflectivity data from multiple radars can be preprocessed into a data format that is efficient for large-scale volumetric visualization in near-real time and requires minimal run-time processing.

Jamison Daniel, David Pugmire, Michael Matheson, Sean Ahern

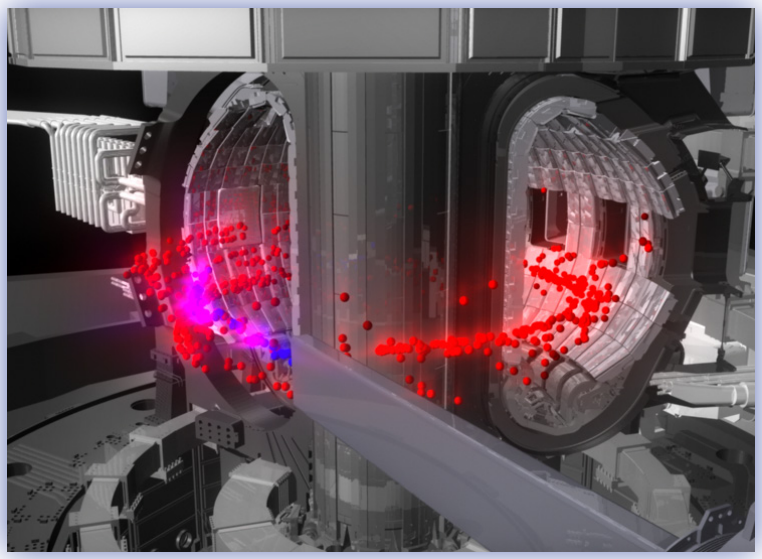

Fusion energy production by alpha particle injection.

Video description:

Within the tokamak, we see field coils, the vacuum vessel, blanket modules, divertor cassettes, and equipment for heating and diagnostics. Visible is one of the high-energy neutral beam injectors that heat and drive the plasma. The fusion fuel consists of deuterium and tritium, which are isotopes of ordinary hydrogen (shown in red and green in the visualization). To produce fusion reactions, the fuel must be heated to a temperature of about one hundred million degrees - about ten times the temperature of the core of the sun. At such temperatures, the electrons of atoms are stripped from the nuclei forming as a state of matter called plasma. One method of achieving these high temperatures is by injecting beams of high-energy neutral atoms into the tokamak. An initial plasma is formed and heated by driving an electric current through the fuel gas in the tokamak chamber. When the plasma reaches a sufficient density and temperature, the injectors are turned on. Because injected atoms are electrically neutral, they are unaffected by the magnetic field and can penetrate deep into the plasma before being ionized by collisions with plasma particles. These very energetic beam ions are trapped by the magnetic field and circulate throughout the plasma, colliding with the plasma particles and transferring energy to them. As the temperature of the plasma rises, due to the beam heating, fusion reactions between the plasma deuterium and tritium begin to occur.

Binary Galaxy Cluster Merger, Simulated using the Flash Code, Mass Ratio 1:1, with an Offset Impact, 4 different views

John Zuhone, Don Lamb

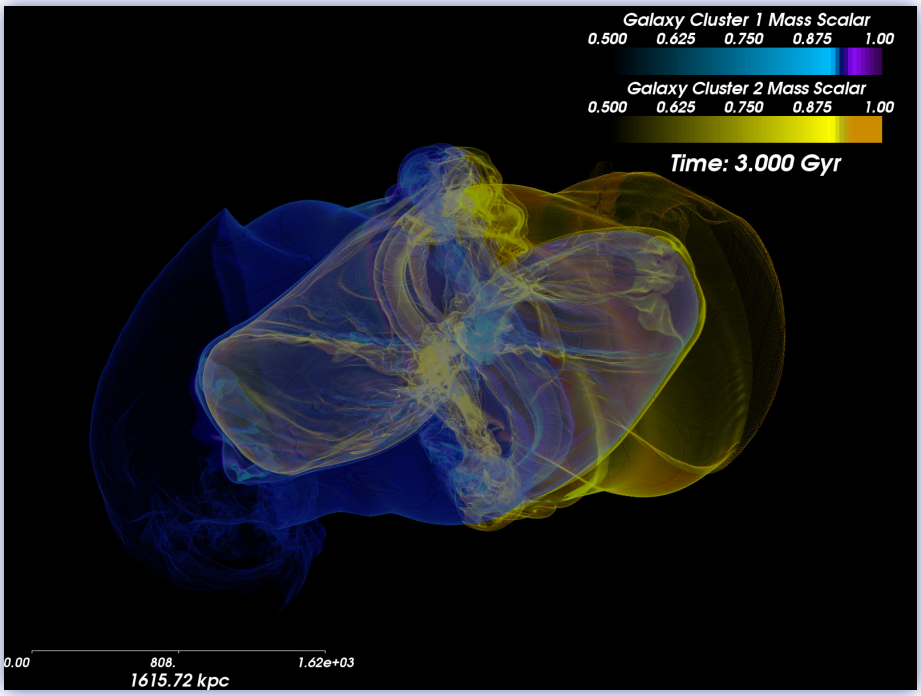

Flash simulation of a Galaxy Cluster merger with a mass ratio of 1:1, and an offset impact. The visualization shows how Dark Matter (visualized as particles) and ordinary matter interact in the merger event.

Video description:

Since structure in the universe forms in a bottom-up fashion, with smaller structures merging to form larger ones, modeling the merging process in detail is crucial to our understanding of cosmology. At the current epoch, we observe clusters of galaxies undergoing mergers. It is seen that the two major components of galaxy clusters, the hot intra-cluster gas and the dark matter, behave very differently during the course of a merger. Using the N-body and hydrodynamics capabilities in the FLASH code, we have simulated a suite of representative galaxy cluster mergers, including the dynamics of both the dark matter, which is collisionless, and the gas, which has the properties of a fluid. 3-D visualizations such as these demonstrate clearly the different behavior of these two components over time.

Dedicated High-End Computing to Revolutionize Climate Modeling: An International Collaboration

B. Doty, D. Achutavarier, J. Adams, E. Altshuler, P. Andrews, B. Cash, B. Huang, E. Jin, J. Kinter, L. Marx, J. Manganello, M. Satoh, C. Stan, D. Straus, H. Tomita

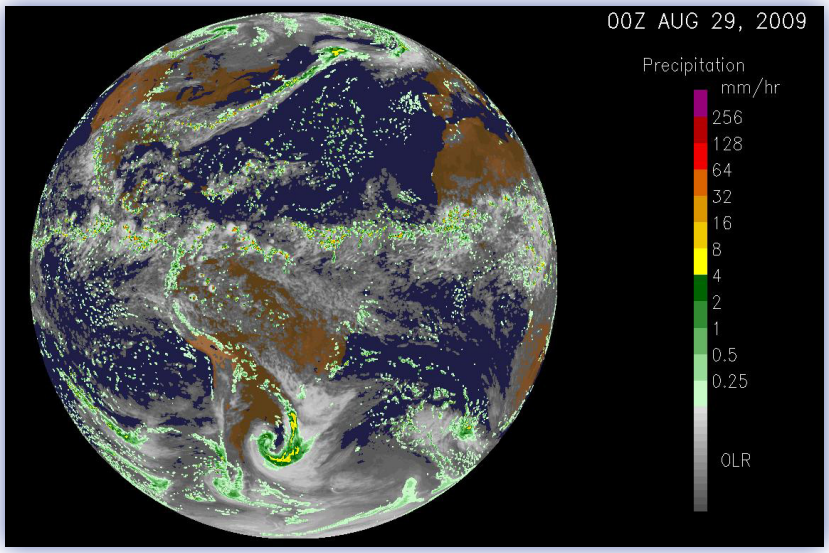

The image is full-disk view of the simulated Earth's atmosphere centered over the Atlantic Ocean. The image depicts the cloudiness (shades of white; based on model-simulated outgoing long-wave radiative flux) and precipitation (colors) at one instant in a long climate simulation of the summer of 2009. Because the model resolution is 7 km, nearly the entire range of multi-scale features in the cloud and rainfall fields can be discerned.

Video description:

The animation depicts a simulation of the Earth's atmosphere, produced from output of a very high-resolution model of the Earth's atmosphere, namely the Non-hydrostatic ICosahedral Atmospheric Model, developed by the University of Tokyo and the Japan Agency for Marine-Earth Science and Technology. The simulation was made as part of a collaboration involving over 30 people, from six institutions on three continents, including climate and weather scientists and modelers, and experts in high-performance computing (HPC), to demonstrate the feasibility of using dedicated resources to rapidly accelerate progress in global climate variability and change. The scientific basis for undertaking this project was established in the World Modeling Summit, held in May 2008 in Reading, UK, where there was a call for a revolution in high-resolution weather and climate modeling. The project made use of the entire 18,048-core Athena Cray XT-4 supercomputer at the University of Tennessee's National Institute for Computational Sciences (NICS).

Visualization of Convective Flow with Integral Surfaces

Christoph Garth, Hari Krishnan, Kenneth I. Joy

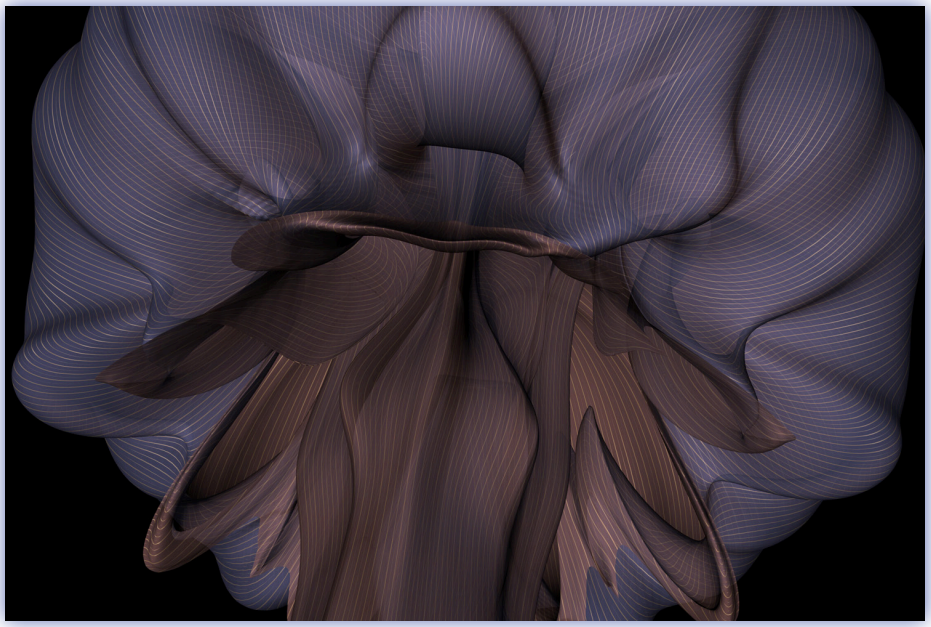

View from below of an integral surface that visualizes a plume-like structure appearing in a convective flow.

Video description:

Integral surfaces are a tool for the visualization of complex flow structures in both steady and unsteady vector fields. These surfaces are derived from the trajectories of massless particles transported by the flow. Depending on how the particles are seeded, different surface types such as path, time, and streak surfaces are obtained. We have developed algorithms to compute such surfaces in a robust and efficient manner, to allow their application to large and complex vector field data. The complex nature of integral surfaces, which can exhibit strong twisting, folding, and shearing, can be problematic in generating a graphical representation that adequately conveys the spatial and temporal characteristics of the flow under consideration. We provide several default approaches to this problem that cover a wide range of integral surface visualization scenarios.

Visualization of a Wind Blade in a Wind Field

Pat Fasel, Jim Ahrens, Jon Woodring, Eunmo Koo, Rod Linn, Judy Wintercamp

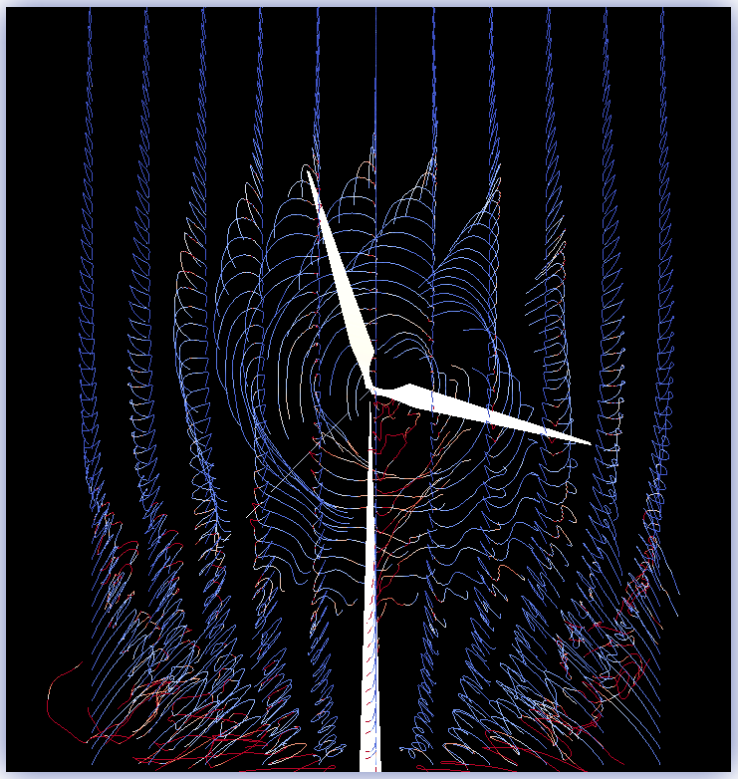

A head on view of a simulated wind blade turning in a wind field.

Video description:

Wind energy is an important key to sustainable, alternative energy sources. In wind farms, the blades turning from a wind source have a non-zero effect on the wind field. Thus, the effects of a wind blade may have impact on the efficiency of other blades in a wind farm. It is important to study these effects to find the optimal wind blade and wind farm configurations. The movie shows a blade turning from a wind source, and also shows the effect of the blade has on the wind field after the blade. The different views show the blade and wind field from the front, side, and top over time. Streamlines depict the change in the instantaneous wind field, which are colored by the wind vorticity. Blue is zero vorticity and red is greater than or equal to 1.0 vorticity.

Web-Enabled Collaborative Climate Visualization

18

Wesley Kendall, Markus Glatter, Jian Huang, Dave Bernholdt, Forrest Hoffman

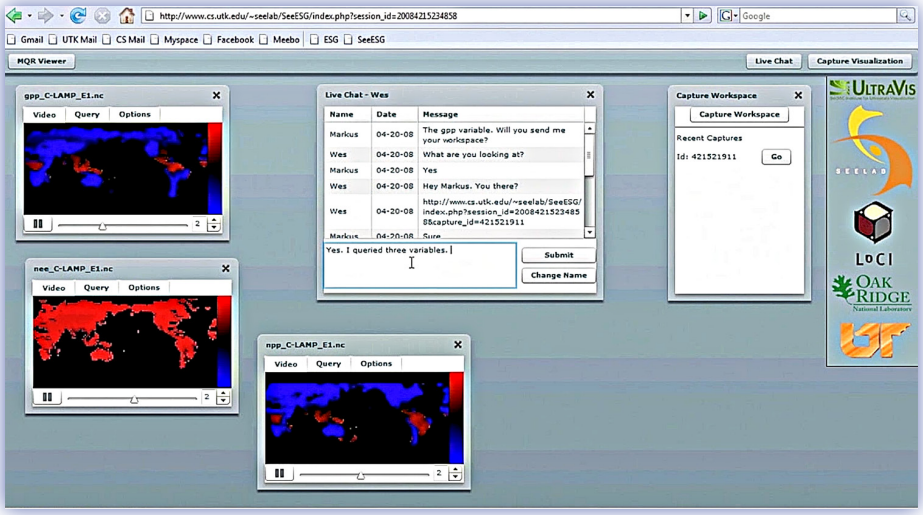

Snapshot of SeeESG, a collaborative interface for querying data from the Earth System Grid.

Video description:

The recent advances in high performance computing, storage and networking technologies have enabled fundamental changes in current climate research. While sharing datasets and results is already common practice in climate modeling, direct sharing of the analysis and visualization process is also becoming feasible. We show our efforts to develop a capability, coupled with the Earth System Grid (ESG), for sharing an entire executable workspace of visualization among collaborators. Evolutionary history of visualizations of research findings can also be captured and shared. The data intensive nature of the visualization system requires using several advanced techniques of visualization and parallel computing. With visualization clients implemented through standard web browsers, however, the ensuing complexity is made transparent to end-users. We demonstrate the efficacy of our system using cutting edge climate datasets.

Comparing Manta Raycaster vs. OpenGL Rendering in ParaView with Metal Ball Splash Data

Li-Ta Lo, John Patchett, Jim Ahrens, Jon Woodring, Dave DeMarle, Nathan Fabian

Manta raycaster rendering in ParaView of a metal ball hitting a metal plate at high velocity.

Video description:

At the petascale and going into exascale, visualization and rendering may be able to run efficiently on the supercomputing platform, rather than relying on visualization clusters with GPUs for rendering. To achieve high-performance rendering with supercomputing nodes, we have tested multi-core software ray-tracing for rendering, such as SCI's Manta raytracer. Initial results show that rendering software optimized for multi-core CPU provides competitive performance to GPU clusters for rendering of large data. Additionally, raytracing can provide additional advanced rendering techniques that basic OpenGL cannot easily provide, such as reflections and shadows. This movie provides a visual comparison between OpenGL rendering and Manta raytracing of a metal ball hitting a metal plate at high velocity, highlighting the advanced shading differences provided by raytracing. The Manta raytracing engine is integrated into VTK and ParaView as a render view, and it provides an alternative to OpenGL on multi-core systems.

CCSM4 HOMME - TMQ (Water Vapor) / Landscan

Jamison Daniel, Mark Taylor, Kate Evans, Eddie Bright

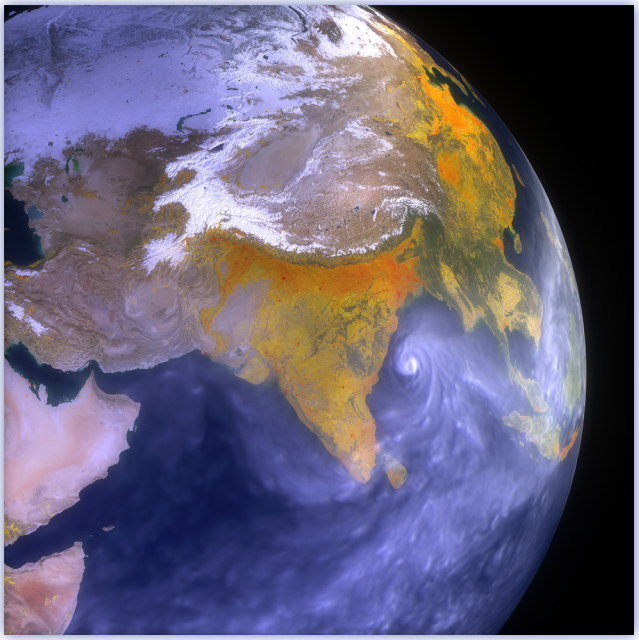

The proper simulation of the distribution of water vapor in the climate system is essential to the accurate treatment of the hydrological cycle and the planetary radiation budget. These images show the simulated monthly-averaged distribution of the total column water vapor from a high-resolution configuration of the CCSM Community Atmospheric Model.

The LandScan Dataset comprises a worldwide population database compiled on a 30 arcsecond by 30 arcsecond latitude/longitude grid. LandScan has been developed as part of the Oak Ridge National Laboratory (ORNL) Global Population Project for estimating ambient populations at risk.

Video description:

HOMME: 1/8 degree resolution; Two-hourly; Two months (Dec. and Jan.). Original cubed-sphere gridded data was interpolated to a grid 25% higher resolution than the original run to avoid interpolation artifacts. CAM 3.5.1 'track 1' physics configuration, but with no surface roughness term in the gravity wave drag parametrization. The data is comprised of instantaneous fields. The LandScan data resolution is 30 arc seconds. The coordinates are Geographic WGS84. The LandScan dataset shown in the visualization is LandScan 2005.

Prabhat, Michael Wehner, Wes Bethel

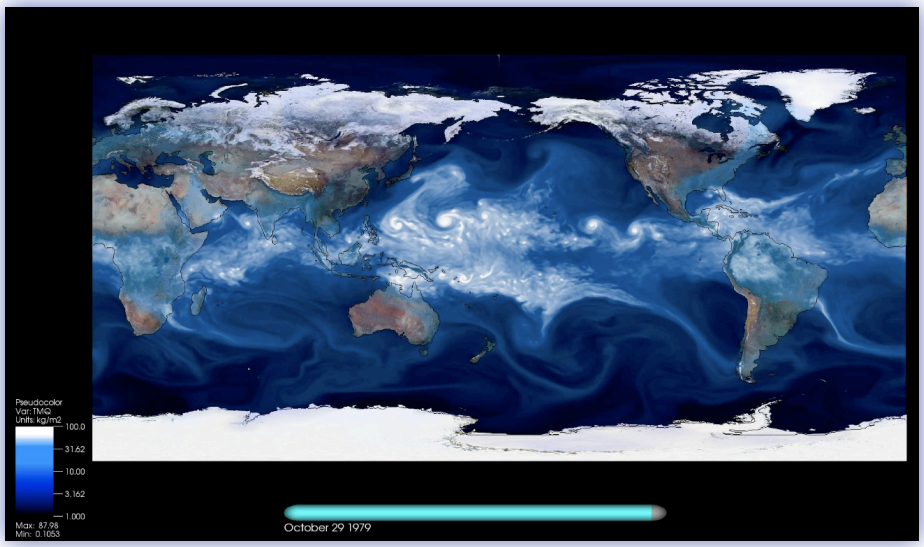

Tropical Cyclone formation and evolution.

Video description:

Global warming will likely change the statistics of tropical cyclones and hurricanes. In this high resolution simulation, using the finite volume version of NCAR's Community Atmosphere Model, we are studying how well the model can reproduce observed tropical cyclone statistics. The simulated storms seen in this animation are generated spontaneously from the model's simulated weather conditions long after the memory of initial conditions have been forgotten. The structure of these simulated tropical cyclones is surprisingly realistic with the strongest storms rating as Category 4 on the Sapphir-Simpson scale. The animated field is the total vertical column integrated water vapor.

Using Simulation and Visualization to Assess Experiment Configuration

A. Obabko, P. Fischer, A. Siegel, S. Lomperski, W. D. Pointer, E. Merzari

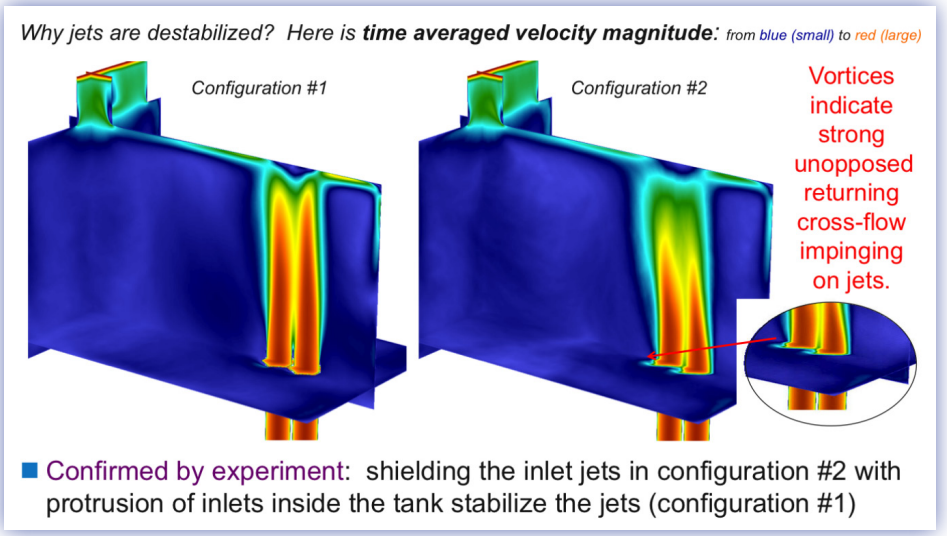

Time averaged velocity magnitude for two configurations of MAX experiment: small protrusion of inlets inside the tank (left) and inlets flushed to the bottom of the tank (right). The simulations and their visualization helped us to discover a jet destabilization mechanism.

Video description:

Using simulations and their visualization of two configurations of MAX experiment helped us to uncover a mechanism for jet destabilization resulted from minor changes in experiment geometry.

The MAX experiment is a mock-up of the upper plenum in sodium cooled fast reactors. It was build at ANL to study gas mixing and heat transfer, and to validate numerical codes for thermal striping problem.

We have conducted numerical simulations of turbulent flow in two different configurations of the experiment with Nek5000 code. The visualization of the simulations with VisIt helped us to discover the physical mechanism that led to destabilization of the inlet jets in the flow after minor changes to experiment configuration.

Our recommendations for stabilization of the flow were successfully implemented in the experiment.

Particle Dynamics in a Fluidized Bed Reactor

Kenny Gruchalla, Perrine Pepiot, Olivier Desjardins

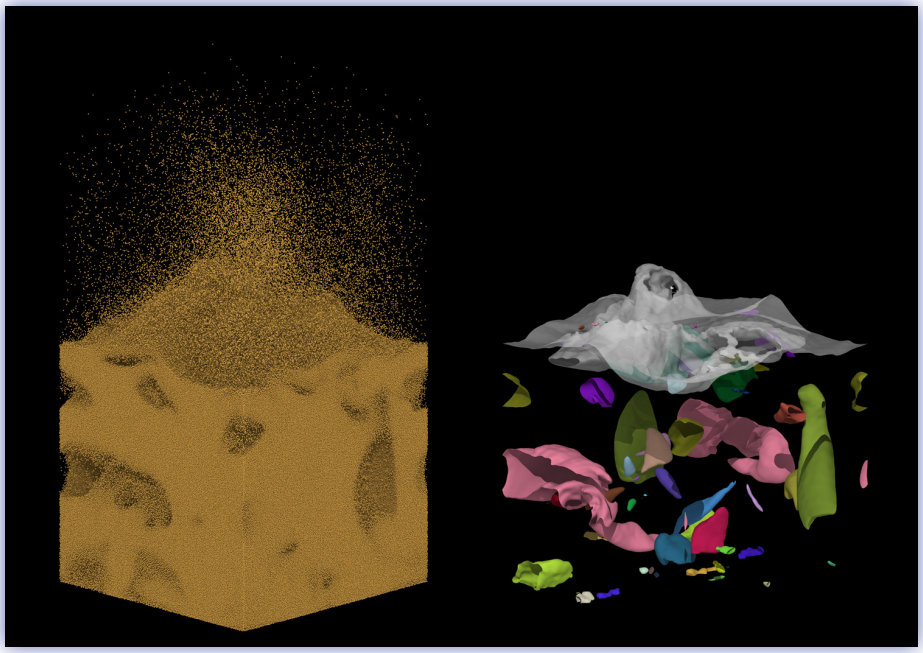

Left: A rendering of a periodic bed of sand fluidized by a gas stream injected from below. Right: Individual bubbles defined by a gas volume fraction of greater than 90% have been extracted and segmented from the particle bed.

Video description:

Fluidized bed reactors are a promising technology for the thermo-chemical conversion of biomass in biofuel production. However, the current understanding of the behavior of the materials in a fluidized bed is limited. We are using high-fidelity simulations to better understand the mechanics of the conversion processes. This video visualizes a simulation of a periodic bed of sand fluidized by a gas stream injected at the bottom. A Lagrangian approach describes the solid phase, in which particles with a soft-sphere collision model are individually tracked along the reactor. A large-scale point-particle direct numerical simulation involving 12 million particles and 4 million mesh points has been performed, requiring 512 cores for 4 days. The onset of fluidization is characterized by the formation of several large bubbles that rise and burst at the surface and is followed by a pseudo-steady turbulent motion showing intense bubble activity.

Visualizing Coolant Flow in Sodium Fast Reactor Subassemblies

Hank Childs, Janet Jacobsen, Paul Fischer, Aleks Obabko

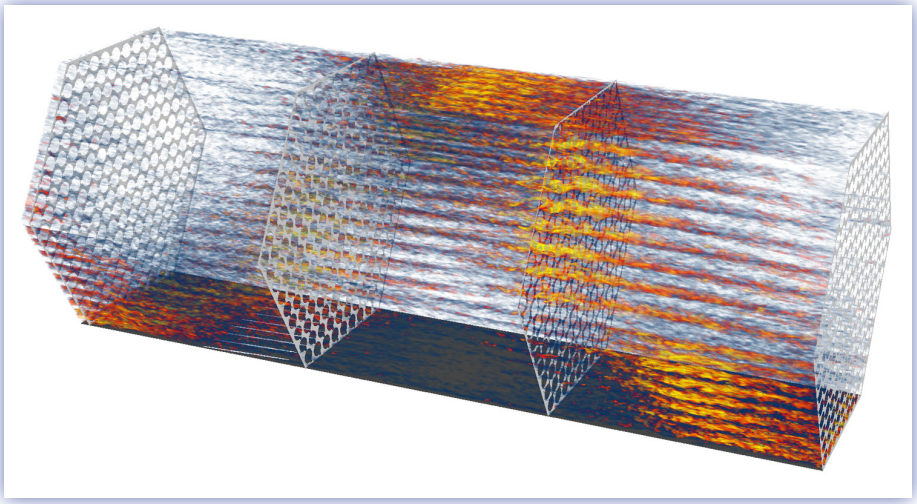

This volume rendering shows areas of high speed (colored yellow and red) through a simulation of a 217 pin reactor on a one billion grid point unstructured mesh.

Video description:

Interchannel cross-flow is the principal cross-assembly energy transport mechanism for sodium fast reactors. For this design, uniform temperatures enable peak power output. This Nek5000 simulation models coolant flow for a 217-pin subassembly, using an unstructured mesh with over one billion grid points, resulting in five billion degrees of freedom per time slice. This visualization of the flow distribution, done with VisIt, provides the type of insight required for improving subassembly designs.

Flash Code Simulation of a University of Michigan High Energy Density Blast-Wave Driven Rayleigh-Taylor Experiment

Nathan Hearn, Tomasz Plewa, Jonathan Gallagher

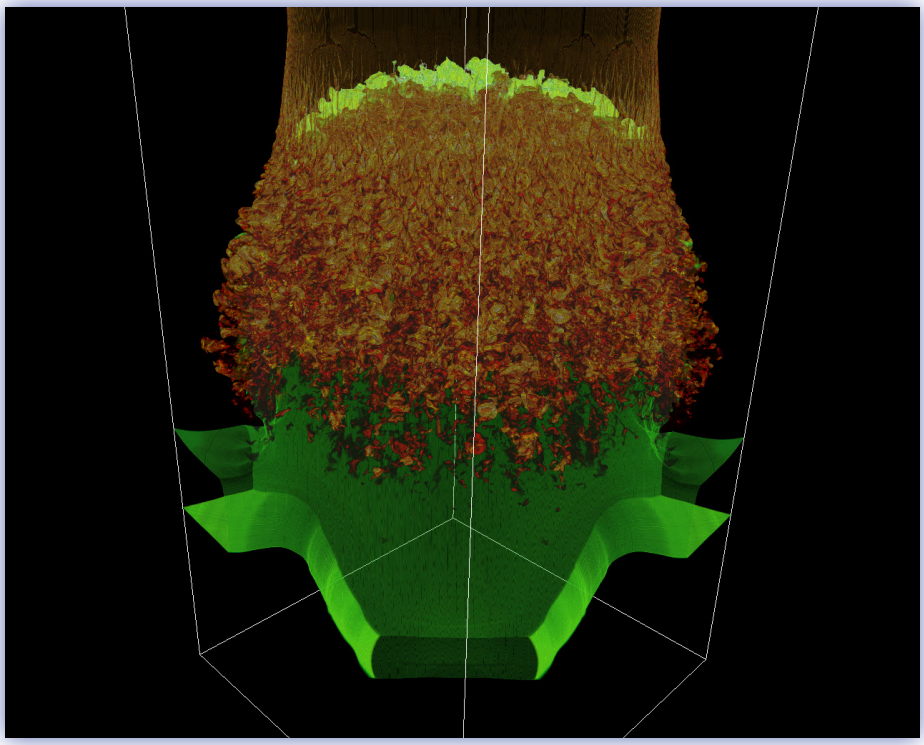

This image shows the simulated growth of instabilities in the dense-to-light interface of the University of Michigan NLUF OMEGA Laser experiment.

Video description:

This movie shows the simulated growth of instabilities in the dense-to-light interface of the University of Michigan NLUF OMEGA Laser experiment. The cylinder is 900 microns in diameter and is resolved to 1.2 microns. The laser input is taken from a 2D, axisymmetric HYADES simulation and mapped onto the Flash code's AMR grid. The duration of the simulation is 20 ns in physical time.

LES of an Inclined Jet into a Supersonic Turbulent Cross-Flow

Antonino Ferrante, Georgios Matheau, Paul Dimotakis, Richard Walters

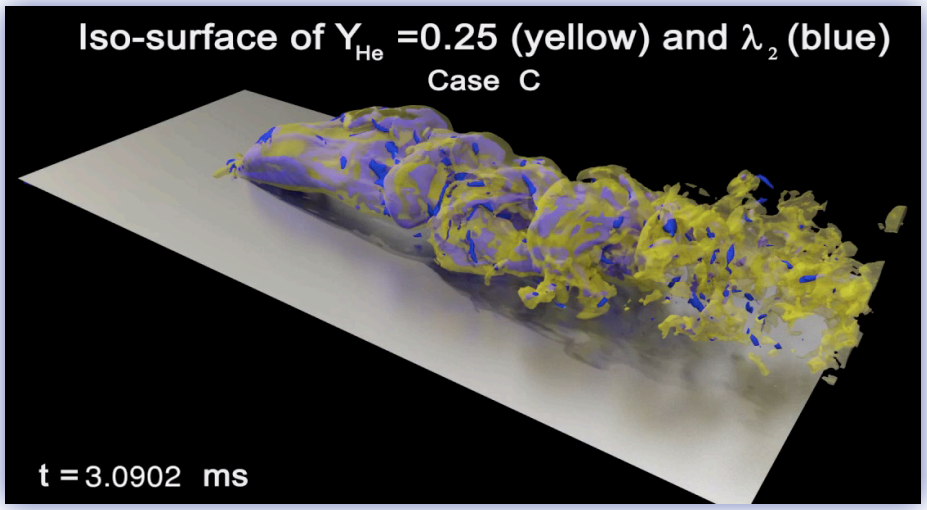

An isosurface of Vorticity computed via Lambda2 combined with He Mass Fraction.

Video description:
A 3.23mm jet injects He into a high velocity flow.

Searching for Baryon Acoustic Oscillations in Intergalactic Absorption, Project StarGate Application Driver

Science
Michael L. Norman, Robert Harkness, Pascal Paschos, Rick Wagner

Visualization
Mark Hereld, Joseph A. Insley, Eric C. Olson, Michael E. Papka

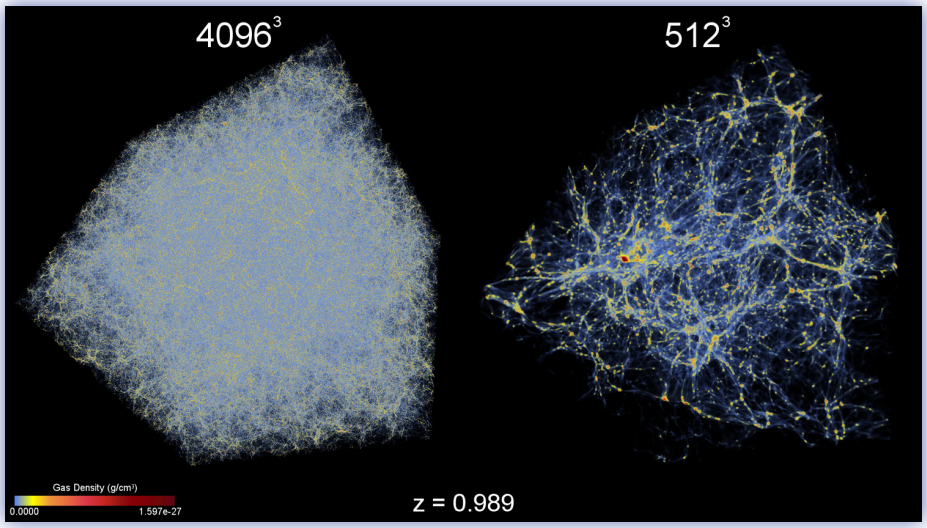

This figure shows side by side views of the full 4096^3 and a 512^3 sub-region of the density field from the baryon acoustic oscillations simulation.

Video description:

This simulation follows the growth of density perturbations in both gas and dark matter components in a volume 1 billion light years on a side beginning shortly after the Big Bang and evolved to half the present age of the universe. It calculates the gravitational clumping of intergalactic gas and dark matter modeled using a computational grid of 64 billion cells and 64 billion dark matter particles. The simulation uses a computational grid of 4096^3 cells and took over 4,000,000 CPU hours to complete.

The visualization shows the density value, whose range spans over 6 orders of magnitude. The animation of the evolution was made from 148 terabytes of data generated on Kraken at the National Institute for Computational Sciences and transferred to Argonne over ESnet. The rendering was performed on Eureka at the Argonne Leadership Computing Facility.

De-crystallization of Cellulose

Gregg T. Beckham, James F. Matthews, Michael F. Crowley

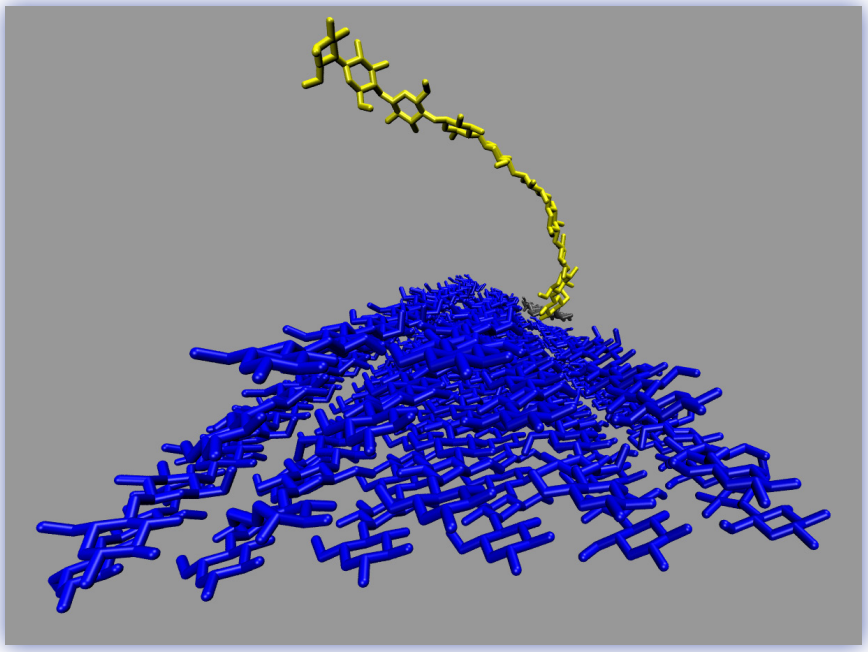

Decrystallization of cellulose simulation as a function of the reaction coordinate.

Video description:

Cellulose-degrading organisms in the biosphere have evolved a complex cocktail of enzymes for overcoming biomass recalcitrance. Most enzyme cocktails contain both processive and non-processive cellulases, which are able to de-crystallize a single cellulose strand and hydrolyze the glycosidic linkages along a cellulose chain. A ubiquitous step that both processive and non-processive cellulases must accomplish is cellulose de-crystallization, for which there is an inherent thermodynamic penalty. Here, we measure the thermodynamic cost for cellulose de-crystallization as a function of cellulose morphology at the atomic scale with molecular simulation. Using molecular dynamics and umbrella sampling we measure the free energy cost of de-crystallizing each cellobiose unit. Our results indicate how enzymes may have evolved to degrade biomass in the biosphere at the molecular-level and suggest directions for increasing the enzymatic accessibility for cellulose digestion in biofuels applications.

Evolution of a Galaxy Cluster in Adaptive Mesh Refinement Cosmological Simulations

Samuel W. Skillman, Brian W. O'Shea, Matthew J. Turk

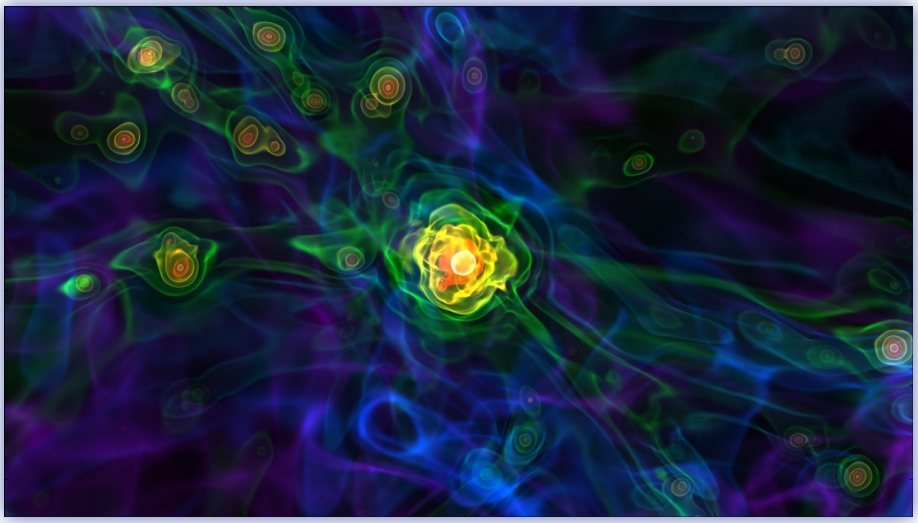

Density isocontours of a galaxy cluster in a cosmological simulation.

Video description:

This movie shows density isocontours of a galaxy cluster during its formation and evolution over 10 billion years. This shows the complex behavior associated with merging clusters, shocks, and virialization.

Effect of Trapped Vortex Combustion with Radial Vane Cavity Arrangements on Predicted Inter-Turbine Burner Performance

30

Balu Sekar, Richard Walters, Kevin George, Miguel Valenciano

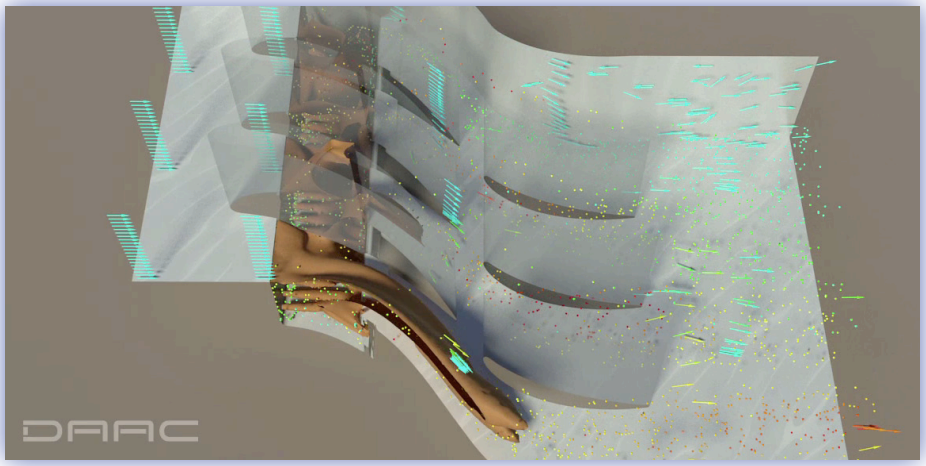

Visualization of flow through the new turbine design.

Video description:
Complex combustion processes, including chemical reactions, turbulence, unsteady, multiphase flow, evaporation and head and mass transfer pose great challenges in modern propulsion system design. AFRL has proposed placing an Ultra-Compact combustor (UCC) between a high pressure turbine stage and low pressure turbine stage to create an innovative Inter-Turbine Burner (ITB) concept. This work focuses on the evaluation of ITB combustor technologies that make use of HPC simulation.

Cellulosomal Enzyme Complex Self-Assembly

Michael F. Crowley, Yannick J. Bomble, Michael E. Himmel

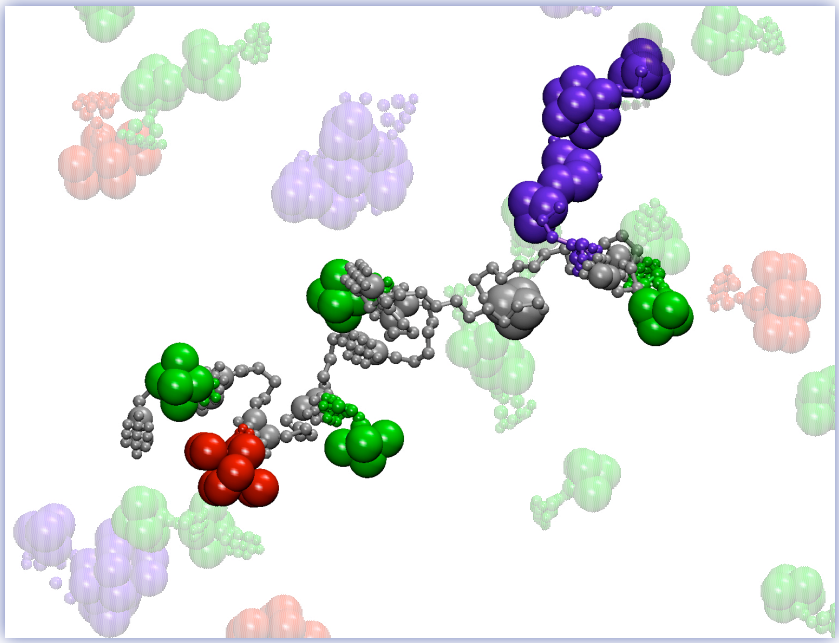

Cellulosomal enzymes assembling on a scaffolding protein. The red, green, and purple groups are different types of enzymatic subunits that bind to the scaffolding and break the bonds of sugar chains in plant cell walls.

Video discription:

Cellulosomes are large multiprotein complexes that can exceed hundreds of millions of atoms in size, making them too massive for atomistic modeling with current computational technologies. Coarser, mesoscale models that describe interactions among structural subunits of the cellulosome rather than individual atoms are used to study cellulosomes. The image shows a mesoscale model of cellulosome assembly developed at NREL and BESC using software developed in SciDAC. The gray "scaffolding" protein forms the structural backbone of this simple cellulosome. The red, green, and purple groups are different types of enzymatic subunits that bind to the scaffolding and break the bonds of sugar chains in plant cell walls. This is a box of sixty enzymes, the ones that bind in the simulation are rendered as solid. [Courtesy of NREL researchers Michael F. Crowley, Yannick J. Bomble, and Michael E. Himmel, National Renewable Energy Laboratory, the BioEnergy Science Center, and SciDAC]

HOMME — Eastern Hemisphere Typhoon Season — Dec/Jan

Jamison Daniel, Mark Taylor, Kate Evans, Jim Hack

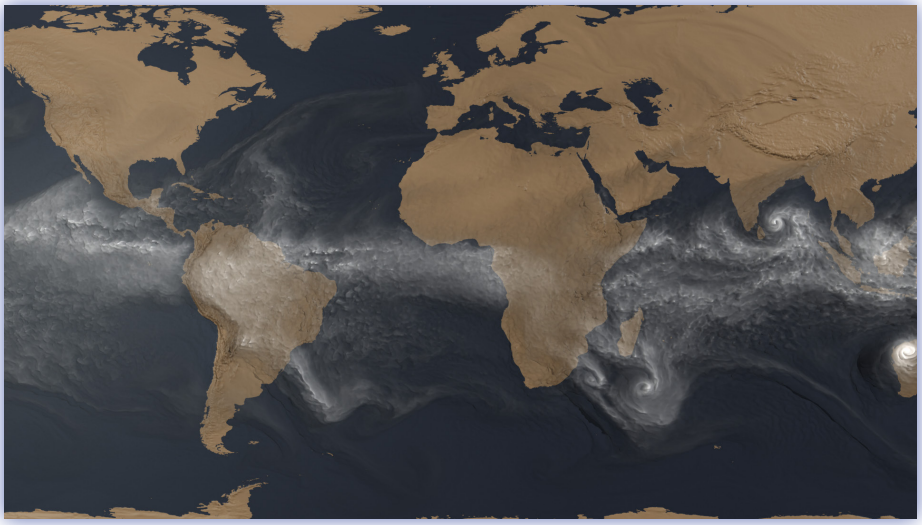
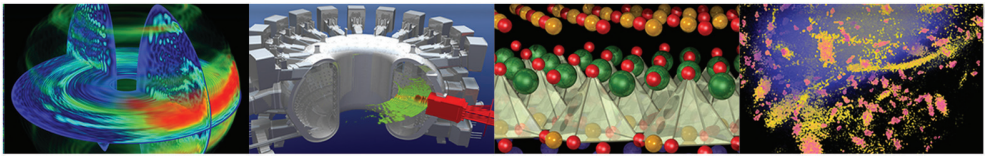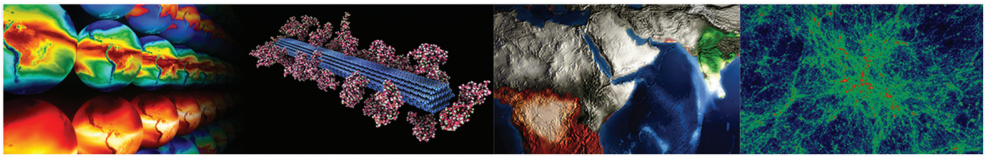
Video description:
Animation of a present day 1/8 degree resolution of columnar precipitable water in the atmosphere. Note that regional features such as cyclones and diurnal precipitation cycles can be discerned at this resolution. This simulation is from CCSM4 with the new spectral element atmospheric dynamical core in a "time-slice" configuration: active atmosphere, land and ice components with prescribed ocean conditions and sea ice extent.